American Mineralogist, Volume 73, pages 1186–1190, 1988

Zimbabweite, $Na(Pb,Na,K)_2As_4(Ta,Nb,Ti)_4O_{18}$, an arsenite-tantalate with a novel corner-linked octahedral sheet

E. N. Duesler
Department of Chemistry, University of New Mexico, Albuquerque, New Mexico 87131, U.S.A.
B. C. Chakoumakos*
Department of Geology, University of New Mexico, Albuquerque, New Mexico 87131, U.S.A.
E. E. Foord
U.S. Geological Survey, M.S. 905, Box 25046, Denver Federal Center, Denver, Colorado 80225, U.S.A.

Abstract

Zimbabweite, $Na(PbNa_{0.5}K_{0.5})As_4(Ta_3Nb_{0.5}Ti_{0.5})O_{18}$, from Karoi District, Zimbabwe, is orthorhombic, $a = 12.245(2)$, $b = 15.287(4)$, $c = 8.684(1)$ Å, $V = 1625.7(5)$ Å^3, space group *Ccmb*, $Z = 4$. The crystal structure has been determined by direct methods and refined by the method of least-squares to an R factor of 0.070, based on 1335 independent reflections measured on an automated single-crystal X-ray diffractometer. The crystal structure, structural formula $M(3)M(2)_2As_4M(1)_4O_{18}$, has a novel bronze-type, corrugated, corner-linked $M(1)_4O_{18}$ octahedral sheet made up of four- and eight-membered octahedral rings parallel to (100). Within the octahedral sheet, a large distorted seven-coordinated site, M(3), is occupied by Na. The octahedral sheets are cross-linked by trigonal-pyramidal arsenite groups and trigonal prisms around M(2), which is occupied by $(PbNa_{0.5}K_{0.5})$. The perfect {010} cleavage breaks the least number of bonds perpendicular to the octahedral sheet, leaving intact, densely packed (010) slabs with cross-linked four-membered octahedral rings. Zimbabweite represents a new structure type.

Introduction

Zimbabweite is a newly described alkali metal–lead arsenite-tantalate from a kaolinized zone of a complex F- and rare-metal-enriched granitic pegmatite at the St. Anns mine, Karoi District, Zimbabwe (Foord et al., 1986). Owing to a lack of any obvious structural relationship to other alkali-metal tantalates or arsenites, a crystal-structure analysis by single-crystal X-ray diffraction was undertaken.

Experimental details

The crystal used in this work is from the original specimen described by Foord et al. (1986), who determined the chemical formula to be $(Na_{1.51}K_{0.48}Ba_{0.04})_{\Sigma 2.03}Pb_{1.01}(As_{4.03}Bi_{0.01})_{\Sigma 4.04}(Ta_{3.17}Nb_{0.55}Ti_{0.26}U_{0.02}Sn_{0.01})_{\Sigma 4.0}O_{18}$. For the purpose of crystal-structure determination, we have assumed an ideal composition of $Na(PbNa_{0.5}K_{0.5})_{\Sigma 2.0}As_4(Ta_3N4b_{0.5}Ti_{0.5})_{\Sigma 4.0}O_{18}$. Several cleavage fragments were examined for imperfections using optical spindle-stage techniques. The chosen crystal (0.069 × 0.115 × 0.161 mm in size) was mounted on a Syntex P3/F automated four-circle diffractometer, and 25 intense reflections were centered using graphite-monochromated Mo$K\alpha$ radiation. Least-squares refinement of the setting angles resulted in the cell dimensions given in Table 1 and an orientation matrix relating the crystal basis to the diffractometer axes. The cell dimensions are in fair agreement with those reported by Foord et al. (1986). To adhere to the convention for orthorhombic crystals that $c < a < b$, the nonstandard space group form *Ccmb* (no. 64) was used. A small data set ($2\theta < 25°$) was collected with no lattice restrictions to test for C-centering. No C-centering violations were observed, and the rest of the data were collected ignoring those absent owing to C-centering. The data were collected using the θ-2θ scan technique. Scan widths ranged from 1.15° below $2\theta(K\alpha_1)$ to 1.25° above $2\theta(K\alpha_2)$, and the scan speeds ranged from 3° to 30°/min. Three standard reflections were collected every 141 reflections. Total background counting time per total scan time was 0.5. The entire sphere of reflection to 62° 2θ was collected and contained 10708 reflections, of which 1348 were unique and allowed by the space group. Of these, 1335 were considered observed at the 3σ level. Maximum and minimum transmission factors were 1.00 and 0.138. An empirical absorption correction based on 360 azimuthal psi scans was applied, along with corrections for Lorentz and polarization effects. A laminar absorption model was used with (001) as the thin face. The agreement among symmetry-equivalent reflections before the absorption correction was 17.37% and after, 4.73%. Because of the high absorption, the intensity data were less than satisfactory.

Structure solution and refinement

Scattering curves for neutral atoms together with anomalous-dispersion corrections were taken from the *International Tables for X-ray Crystallography* (Ibers and Hamilton, 1974). The SHELXTL system of programs (Sheldrick, 1981) was used for the computations. The R indices are of the form given in Table 1.

* Present address: Solid State Division, Bldg. 2000, Oak Ridge National Laboratory, P.O. Box 2008, Oak Ridge, Tennessee 37831-6056, U.S.A.

0003–004X/88/0910–1186$02.00

TABLE 1. Crystal and data collection summary for zimbabweite

a	12.245(2) Å	Crystal size (mm)	0.069 × 0.115 × 0.161
b	15.287(4) Å	λ MoKα (Å)	0.71069
c	8.684(1) Å	Total $\|F_o\|$	1348
V	1625.6(5) Å^3	$\|F_o\| > 3\sigma$	1335
μ (MoKα)	403.8 cm^{-1}	Final R(obs)	7.07%
D_{calc}	5.97 g/cm^3	$R = \Sigma(\|F_o\| - \|F_c\|)/\Sigma\|F_o\|$	
		Final R_w(obs)	7.22%
		$R_w = [\Sigma w(\|F_o\| - \|F_c\|)^2/\Sigma F_o^2]^{1/2}$	
		$w = 1/[\sigma^2(F_o) + \|g\|F_o^2]$	
		$g = 0.0045$	

Space group *Ccmb* (no. 64)
Origin at 0.25**a** + 0.25**b** with respect to the *International Tables for Crystallography* (Hahn, 1983).
Unit-cell contents: $4[Na(PbNa_{0.5}K_{0.5})As_4(Ta_3Nb_{0.5}Ti_{0.5})O_{18}]$

The structure was solved by direct methods. The best E map gave trial positions for four heavy atoms. Refinement based on these gave an R factor of 40%. A difference map showed the positions for the other atoms. The idealized chemical composition was changed for several block cascade, least-squares refinements, which successfully improved the model. The final model included anisotropic temperature factors for all atoms; M(1) sites are occupied by 75% Ta, 12.5% Nb, and 12.5% Ti, and the M(2) sites are occupied by 50% Pb, 25% K, and 25% Na. This model (72 parameters) in space group *Ccmb* converged to an R index of 7.0% (observed) and an R_w index of 7.2% (observed). Refinement of the model in the noncentric space group *Cc2a* did not improve the agreement. The final positional parameters are given in Table 2, anisotropic temperature factors in Table 3, and selected interatomic distances and angles in Tables 4 and 5. A bond valence analysis is given in Table 6. Observed and calculated structure factors are given in Table 7.[1]

STRUCTURE DESCRIPTION

The M(1) site is coordinated by an octahedral arrangement of oxygens and is occupied by 75% Ta, 12.5% Ti, and 12.5% Nb. The M(1) octahedra are corner-linked into infinite M_8O_{36} sheets consisting of four- and eight-membered octahedral rings (Fig. 1). The octahedral sheets are corrugated and parallel to (100). Atoms O(4), O(5), and O(6) are bridging oxygens within the octahedral sheet, and their bond lengths to the M(1) cation are shorter (0.08 Å on average) than the nonbridging oxygen–M(1) bonds (Table 4). The interoctahedral M(1)–O_{br}–M(1) angles are 165.6(4)°, 171.1(2)°, and 163.5(4)°, involving O(4), O(5), and O(6), respectively.

Within the octahedral sheet is a large metal site, M(3), with a distorted cubic coordination centered within the eight-membered ring. This site is occupied by Na. The octahedral layers are cross-linked by As^{3+} in typical trigonal-pyramidal coordination and by an additional large metal site, M(2), with distorted trigonal-prismatic coordination. The M(2) sites are occupied by 50% Pb, 25% Na, and 25% K. The geometries of the M(2) and M(3) coordination polyhedra are illustrated in Figure 2. The M(3) site has eight oxygen neighbors within 2.75 Å, forming a highly distorted cubic arrangement. The coordination number of M(3) increases to 10 if the weak bond to the O(4) oxygen at a distance of 2.91(2) Å is included, which adds two caps to the distorted, cubic, polyhedral coordination. The geometery of the arsenite trigonal pyramid is in fair agreement with the average structure of 27 arsenite groups in 12 minerals (Hawthorne, 1985; Ghose et al., 1987). The lone pair of electrons on each As^{3+} cation is roughly directed along the **a** direction away from the nearest M(3) site, and the plane defined by the oxygens of the arsenite group roughly parallels (010) (Figs. 1a and 1c).

[1] To obtain a copy of Table 7, order Document AM-88-389 from the Business Office, Mineralogical Society of America, 1625 I Street, N.W., Suite 414, Washington, D.C. 20006, U.S.A. Please remit $5.00 in advance for the microfiche.

TABLE 2. Atom coordinates and equivalent isotropic temperature factors* for zimbabweite

Atom**	Position†	x/a	y/b	z/c	U_{eq} (Å^2)*
M(1)	16g 1	0.81379(4)	0.37712(4)	0.30173(7)	0.0100(2)
M(2)	8f *m*	0.4504(1)	¼	0.8793(2)	0.0202(3)
M(3)	4b 2/*m*	¾	¼	0	0.033(4)
As	16g 1	0.5855(1)	0.42180(8)	0.0686(2)	0.0132(3)
O(1)	16g 1	0.6669(9)	0.3660(8)	0.205(1)	0.020(3)
O(2)	16g 1	0.1188(9)	0.3535(7)	0.586(1)	0.020(3)
O(3)	16g 1	0.9639(8)	0.3642(7)	0.386(1)	0.019(3)
O(4)	8f *m*	0.805(1)	¼	0.326(2)	0.020(4)
O(5)	8e 2	0.826(1)	½	¼	0.019(4)
O(6)	8d 2	¾	0.395(1)	½	0.016(3)

Note: Standard deviations of the last digit are in parentheses.
* Equivalent isotropic U defined as one-third of the trace of the orthogonalized U tensor.
** M(1) = 75% Ta, 12.5% Nb, 12.5% Ti. M(2) = 50% Pb, 25% K, 25% Na. M(3) = 100% Na.
† Multiplicity, Wyckoff position, and point symmetry of site.

TABLE 3. Anisotropic-temperature-factor coefficients, U_{ij} (in Å^2 × 10^4) for zimbabweite

Atom	U_{11}	U_{22}	U_{33}	U_{23}	U_{13}	U_{12}
M(1)	105(3)	102(3)	92(4)	6(2)	3(2)	3(2)
M(2)	137(5)	224(6)	245(7)	76(5)	0(0)	0(0)
M(3)	24(6)	29(6)	47(9)	15(6)	0(0)	0(0)
As	118(5)	139(6)	138(6)	3(4)	1(4)	4(4)
O(1)	28(5)	21(4)	10(5)	5(4)	0(4)	2(4)
O(2)	17(4)	32(5)	10(4)	1(4)	−1(3)	0(4)
O(3)	22(5)	15(4)	20(5)	4(3)	−1(4)	2(4)
O(4)	20(7)	12(6)	28(6)	0(5)	0(0)	0(0)
O(5)	15(6)	30(7)	13(6)	0(0)	1(5)	0(0)
O(6)	22(6)	21(6)	3(5)	−1(4)	0(0)	0(0)

Note: Standard deviations of the last digit are in parentheses.

TABLE 4. Selected bond lengths (Å) in zimbabweite

As–O(1)	1.77(1)	M(2)–O(1)e, f	2.73(1) ×2
As–O(2)	1.75(1)	M(2)–O(2)c, e	2.61(1) ×2
As–O(3)	1.77(1)	M(2)–O(3)a, b	2.68(1) ×2
Mean	1.76	Mean	2.67
M(1)–O(1)	1.99(1)	M(3)–O(1)a, b, c, d	2.71(1) ×4
M(1)–O(2)	2.07(1)	M(3)–O(2)b, c, d, e	2.37(1) ×4
M(1)–O(3)	1.99(1)	Mean	2.54
M(1)–O(4)	1.958(2)		
M(1)–O(5)	1.938(1)		
M(1)–O(6)	1.911(2)		
Mean	1.97		

Note: Standard deviations of the last digit are in parentheses. The letters a–f appended to O(1) to O(3) refer to symmetry-equivalent atom labels.

The bond-valence sums (in valence units, v.u.) to the cation sites, 3.17 for As, 4.90 for M(1), 1.18 for M(2), and 1.16 for M(3), agree reasonably well with the mean formal valences of the cations at those sites, 3.0, 4.875, 1.50, and 1.0, respectively (Table 6), with the exception of M(2). The bridging oxygens, O(4), O(5), and O(6) within the octahedral sheet, are all underbonded with respect to their ideal bond-valence sums of 2.0 v.u., O(4) and O(5) being notably deviant in this respect. Addition of the M(3)–O(4) bonds and weak M(3) interactions at 3.11 Å and 3.16 Å increases the O(4) bond-valence sum to a reasonable 1.95 v.u. Small amounts of U^{6+} may substitute at the M(1) site [Foord et al. (1986) reported 0.3 wt% UO_2], and this substitution would further improve the valence sums to O(4), O(5), and O(6). Thermogravimetric, F, and water analyses (Foord et al., 1986) yielded only minor H_2O (0.13 wt%) and F (0.04 wt%), which might offer alternative explanations had more been detected.

Despite the conspicuous octahedral sheet in zimbabweite, the perfect {010} cleavage of the mineral likely

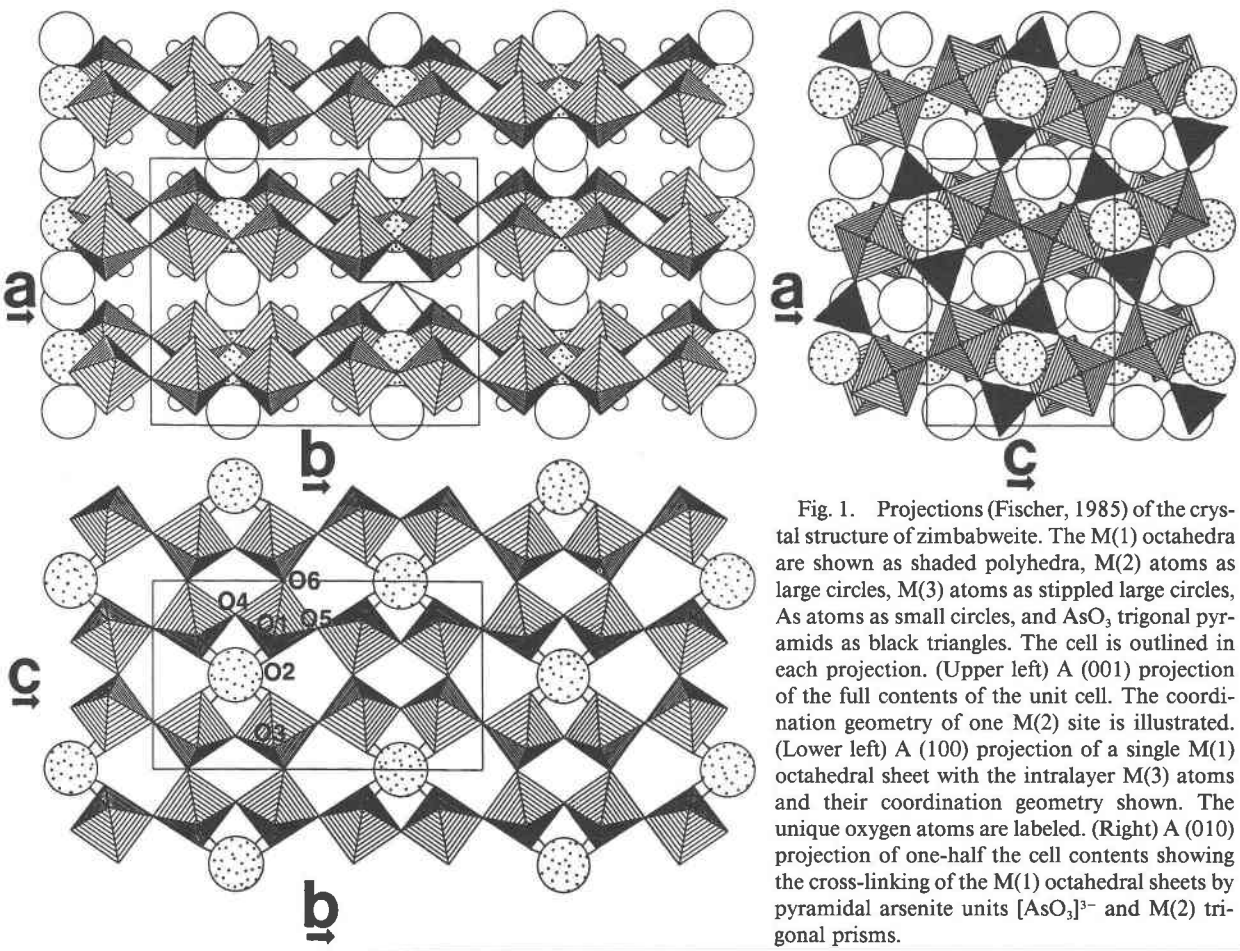

Fig. 1. Projections (Fischer, 1985) of the crystal structure of zimbabweite. The M(1) octahedra are shown as shaded polyhedra, M(2) atoms as large circles, M(3) atoms as stippled large circles, As atoms as small circles, and AsO_3 trigonal pyramids as black triangles. The cell is outlined in each projection. (Upper left) A (001) projection of the full contents of the unit cell. The coordination geometry of one M(2) site is illustrated. (Lower left) A (100) projection of a single M(1) octahedral sheet with the intralayer M(3) atoms and their coordination geometry shown. The unique oxygen atoms are labeled. (Right) A (010) projection of one-half the cell contents showing the cross-linking of the M(1) octahedral sheets by pyramidal arsenite units $[AsO_3]^{3-}$ and M(2) trigonal prisms.

TABLE 5. Polyhedral edge lengths (Å) and angles (°) in zimbabweite

Trigonal-pyramidal arsenite polyhedron			
O(1)–O(3)a	2.61(2)	O(1)–As–O(3)a	95.0(5)
O(1)–O(2)a	2.61(1)	O(1)–As–O(2)a	95.7(5)
O(3)a–O(2)a	2.57(2)	O(3)a–As–O(2)a	93.9(5)
Mean	2.60	Mean	94.8
Octahedral M(1) polyhedron			
O(1)–O(4)	2.66(2)	O(1)–M(1)–O(4)	84.9(5)
O(1)–O(5)	2.85(2)	O(1)–M(1)–O(5)	93.4(5)
O(1)–O(6)	2.78(1)	O(1)–M(1)–O(2)a	88.1(4)
O(1)–O(2)a	2.82(2)	O(4)–M(1)–O(2)a	86.9(6)
O(4)–O(3)	2.66(2)	O(3)–M(1)–O(6)	93.3(6)
O(4)–O(6)	2.76(2)	O(5)–M(1)–O(6)	95.6(5)
O(4)–O(2)a	2.77(2)	O(1)–M(1)–O(6)	91.2(3)
O(3)–O(5)	2.92(1)	O(4)–M(1)–O(3)	84.9(5)
O(3)–O(6)	2.83(1)	O(4)–M(1)–O(6)	91.4(7)
O(3)–O(2)a	2.80(2)	O(3)–M(1)–O(5)	96.2(5)
O(5)–O(6)	2.85(1)	O(3)–M(1)–O(2)a	87.1(4)
O(5)–O(2)a	2.73(1)	O(5)–M(1)–O(2)a	85.9(3)
Mean	2.79	Mean	89.9
Distorted trigonal-prismatic M(2) polyhedron			
O(3)b–O(1)a	3.88(2) ×2	O(3)b–M(2)–O(1)a	91.6(3) ×2
O(3)b–O(2)b	2.57(2) ×2	O(1)a–M(2)–O(2)b	94.8(3) ×2
O(1)a–O(2)b	3.94(2) ×2	O(3)b–M(2)–O(2)b	58.2(3) ×2
O(3)b–O(3)a	3.49(2)	O(3)b–M(2)–O(3)a	81.2(5)
O(1)a–O(1)b	3.54(2)	O(1)a–M(2)–O(1)b	80.8(5)
O(2)b–O(2)a	3.16(2)	O(2)b–M(2)–O(2)a	74.4(5)
Distorted cubic M(3) polyhedron			
O(1)b–O(1)d	3.54(2) ×2	O(1)b–M(3)–O(1)d	81.5(5) ×2
O(2)b–O(2)d	3.16(2) ×2	O(2)d–M(3)–O(2)b	83.5(5) ×2
O(1)b–O(2)b	2.82(2) ×4	O(1)b–M(3)–O(2)b	67.0(4) ×4
O(1)b–O(2)c	2.61(1) ×4	O(1)b–M(3)–O(2)c	61.4(3) ×4
Mean	2.93	Mean	70.3

Note: Standard deviations of the last digit are in parentheses. The letters a–f appended to O(1) to O(3) refer to symmetry-equivalent atom labels.

TABLE 6. Empirical bond-valence table for zimbabweite

	As	M(1)	M(2)	M(3)	Σ
O(1)	1.04	0.78	0.17 ×2↓	0.09 ×4↓	2.08
O(2)	1.09	0.64	0.23 ×2↓	0.20 ×4↓	2.16
O(3)	1.04	0.78	0.19 ×2↓		2.01
O(4)		0.85 ×2→			1.70
O(5)		0.89 ×2→			1.78
O(6)		0.96 ×2→			1.92
Σ	3.17	4.90	1.18	1.16	

Note: Weighted-average bond valences in valence units calculated from the curves of Brown (1981).

occurs along the planes defined by the O(5) oxygens perpendicular to the octahedral sheets, as the fewest number of bonds are broken in this manner and densely packed (010) slabs with cross-linked four-membered octahedral rings remain intact (Fig. 1).

The octahedral layer in zimbabweite is a new member of the class of corner-linked octahedral sheets characterized by the so-called bronzes (see Megaw, 1973). Figure 3 compares the zimbabweite sheet with three other important corner-linked octahedral sheets: perovskite, hexagonal tungstsen bronze (htb), and tetragonal tungsten bronze (ttb).

That the mean M(1)–O_{br} bond length is shorter than the M(1)–O_{nbr} bond length in zimbabweite is contrary to our experience with Si–O bonds in polymerized silicate anions. In silicates, Si–O_{br} bonds are, on average, 0.025 Å longer than Si–O_{nbr} bonds (Liebau, 1985). What should be expected for corner-sharing MO_6 octahedral anions? First, we should restrict our attention to those structures with octahedral anions with corner-sharing only and exclude those that are infinite three-dimensional frameworks (e.g., htb and ttb), which would lack M–O_{nbr} bonds. An exhaustive survey of these kinds of structures has not been made, but the mineral groups alunite, beudantite, and crandallite all possess a corner-linked octahedral sheet based on three- and six-membered octahedral rings as in the htb structure. For these three mineral groups, the octahedral-sheet cations are Al, Fe^{3+}, or Cu^{2+}, and for each mineral whose structure has been refined, the M–O_{br} bonds are shorter than the M–O_{nbr} bonds. Note that in the octahedral sheet that characterizes these mineral groups, the bridging oxygen is actually a hydroxyl, whereas the nonbridging oxygens are not. Indeed, for a formal valence of +3 or less on the metal cation, an additional bond to the bridging oxygen is required to satisfy the electrostatic neutrality principle. Apparently, when pentavalent cations occupy a corner-linked octahedral anion, as in zimbabweite, a slight amount of underbonding to the bridging oxygens can be tolerated. Another exceptional compound, $Ba_3Si_4Ta_6O_{26}$, whose structure was determined by Shannon and Katz (1970), allows the comparison of bridging versus nonbridging bonds in both a silicate anion and a corner-linked TaO_6 octahedral anion. This structure contains rings of three TaO_6 octahedra sharing corners, which are stacked in columns by corner-linking. These columns are cross-linked by disilicate groups. The Ba occupies channelways between the columns of octahedra and is mainly bonded to the nonbridging oxygens with weak interactions to the bridging oxygens in the columns of octahedra. In this structure, the mean Si–O_{br} bond [1.66(6) Å] is longer than the mean Si–O_{nbr} bond [1.61(4) Å], as observed in other silicates, whereas the mean Ta–O_{br} bond [1.94(3) Å] is shorter than the mean Ta–O_{nbr} bond [2.04(3) Å], as observed in the alunite-type sheet. We must conclude that corner-linked octahedral linkages are unlike silicates in terms of their bridging versus nonbridging bond lengths. Zimbabweite is apparently typical of other structures with corner-linked octahedral anions, but we hesitate to say that all M–O_{br} bonds are longer than M–O_{nbr} bonds

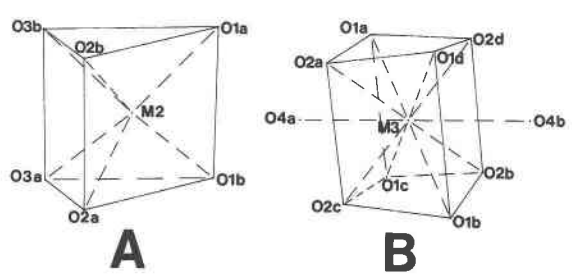

Fig. 2. Coordination polyhedra for (A) the distorted trigonal prismatic M(2) site (*m* point symmetry) and (B) the distorted cubic M(3) site (2/*m* point symmetry).

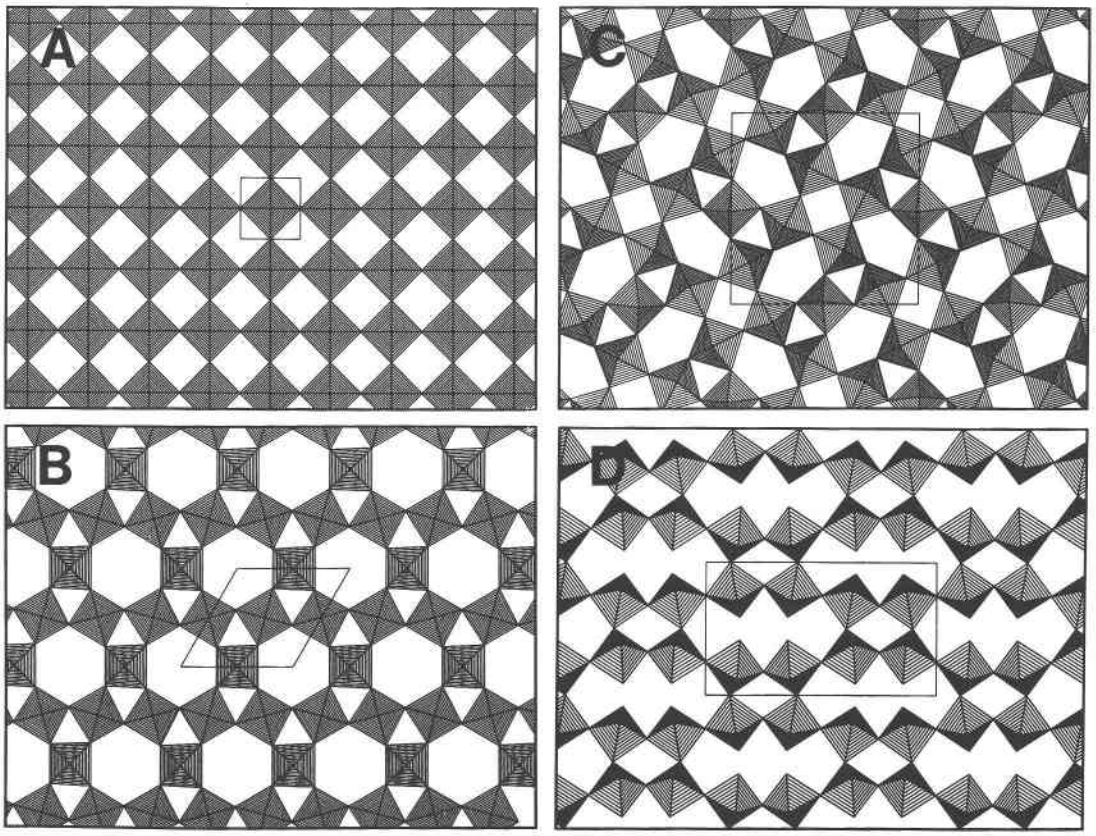

Fig. 3. Comparison of corner-linked octahedral sheets. Unit cells are outlined for each sheet. (**A**) The perovskite (or more properly K_2NiF_4) sheet, which consists of four-membered octahedral rings. (**B**) The hexagonal tungsten bronze (htb) sheet (the fundamental building unit in the alunite group minerals), which consists of three- and six-membered octahedral rings. (**C**) The tetragonal tungsten bronze (ttb) sheet, which consists of three-, four- and five-membered octahedral rings. (**D**) The zimbabweite octahedral sheet, which consist of four- and eight-membered octahedral rings.

in corner-linked octahedral anions until more structures are examined.

Acknowledgments

We thank Joan Fitzpatrick, Richard C. Erd, Howard T. Evans, and Subrata Ghose for thoughtful reviews of the manuscript. This work was supported in part by the U.S. Department of Energy, Basic Energy Sciences under grant DE-FG04-84ER45099 (Principal Investigator, R. C. Ewing, University of New Mexico).

References cited

Brown, I.D. (1981) The bond-valence method: An empirical approach to chemical structure and bonding. In M. O'Keeffe and A. Navrotsky, Eds., Structure and bonding in crystals, vol. 2, p. 1–30. Academic Press, New York.

Fischer, R.X. (1985) STRUPLO84, a Fortran plot program for crystal structure illustrations in polyhedral representation. Journal of Applied Crystallography, 18, 258–262.

Foord, E.E., Taggart, J.E., Jr., Gaines, R.V., Grubb, P.L.C., and Kristiansen, R. (1986) Zimbabweite, a new alkali-lead-arsenic tantalate from St. Anns Mine, Karoi District, Zimbabwe. Bulletin de Minéralogie, 109, 331–336.

Ghose, S., Sen Gupta, P.K., and Schlemper, E.O. (1987) Leiteite, $ZnAs_2O_4$: A novel type of tetrahedral layer structure with arsenite chains. American Mineralogist, 72, 629–632.

Hahn, T., Ed. (1983) International tables for crystallography. D. Reidel, Boston.

Hawthorne, F.C. (1985) Schneiderhöhnite, $Fe^{2+}Fe^{3+}{}_3As^{3+}{}_5O_{13}$, a densely packed arsenite structure. Canadian Mineralogist, 23, 675–679.

Ibers, J.A., and Hamilton, E.C., Eds. (1974) International tables for X-ray crystallography, Vol. 4. Kynoch Press, Birmingham, England.

Liebau, F. (1985) Structural chemistry of silicates, p. 17–19. Springer-Verlag, New York.

Megaw, H.D. (1973) Crystal structures, a working approach, p. 329–332. McGraw-Hill, New York.

Shannon, J., and Katz, L. (1970) The structures of the reduced oxidized forms of barium silicon tantalum oxide, $Ba_3Si_4Ta_6O_{23}$ and $Ba_3Si_4Ta_6O_{26}$. Journal of Solid State Chemistry, 1, 399–408.

Sheldrick, G.M. (1981) SHELXTL: A programme for crystal structure determination. Institut für Anorganische Chemie der Universität, Gottingen, FRG.

Manuscript received November 30, 1987
Manuscript accepted May 25, 1988